Preprint
UCRL-JC-137881

On the Elasto-Plastic Response of a Large-Tow Triaxial Braided Composite

E. Zywicz, M.J. O'Brien, T. Nguyen

This article was submitted to
15th Annual Technical Conference, American Society for Composites, College Station, TX, September 24-27, 2000

June 14, 2000

On the Elasto-Plastic Response of a Large-Tow Triaxial Braided Composite

By

Edward Zywicz,
Michael J. O'Brien,
and
Thao Nguyen

ABSTRACT

The elastic-plastic response of a large-tow $0^o/\pm\theta^o$ tri-axially braided composite is numerically simulated to determine the elastic coefficients and post-yield behavior. The ratios of extensional to flexural effective Young's moduli vary from 0.30 to 0.52 in the longitudinal direction and 0.90 to 0.95 in the transverse direction. Measurements on a 2-ply $0^o/\pm 30^o$ braid support these numerical trends. The onset of macro yield in uniaxial extension coincides with the experimental values in the longitudinal direction while it is nearly twice the experimental values in the transverse direction. In simple shear, matrix plasticity around the undulations facilitates local rotation of the braiders at the onset of macro yield. Under uniaxial flexure, modest stiffening occurs prior to strain softening in both the principal directions.

INTRODUCTION

Due to fiber undulations present in woven and braided composites, the effective lamina flexural and extensional properties are distinct quantities not derivable from one another. Marrey and Sankar [1] calculated the extensional, bending, and coupling matrices for a plain weave and a five-harness satin weave textile composite plate using representative volume elements (RVEs) and periodic boundary conditions, and showed that the extensional matrix could not be used to construct either the bending or coupling matrices. Whitcomb et al. [2] used finite

[1] Zywicz and O'Brien – University of California, Lawrence Livermore National Laboratory, PO Box 808, Livermore, CA 94556 USA

[2] Nguyen – presently at Stanford University, Mechanical Engineering, Stanford, CA 94305 USA

elements (FE) to examine a plain weave composite subjected to flexure and explored how free surfaces influence the effective stiffness. Based upon lamination theory, they developed an expression for E_{lam}, the effective flexural modulus of the laminate, given by

$$\frac{E_{lam}}{E} = \frac{E_{flex}}{E}\frac{1}{n^2} + \left(1 + \frac{1}{n^2}\right), \tag{1}$$

where n is the number of RVEs in the laminate, and E_{flex} and E are the effective lamina flexural and extensional Young's moduli, respectively. Zywicz and Nguyen [3] employed the FE method to determine the effective plane-stress extensional and flexural properties of a $0^o/\pm 30^o$ tri-axially braided composite lamina. The flexural Young's moduli were calculated to be just 0.52 and 0.92 of their extensional counterparts in the longitudinal and transverse directions, respectively. Measurements performed on a 2-ply system were in general agreement with their FE predictions. They concluded that in systems that contain relatively few laminae, e.g., large tow composites, or where delamination generates sub-laminates with few laminae, it is important to use the independent effective flexural and extensional properties.

While the elastic behavior of textile composites with polymeric matrices has received substantial attention, less emphasis has been directed on the pre-damage nonlinear response of these materials. In part, this is due to the assumption, which may or may not be correct, that damage is primarily responsible for the nonlinear behavior experimentally observed.

This paper extends the previous work of [3] in two directions. First, it analyzes additional, geometrically similar, triaxial braids to determine how the ratio of flexural to extensional elastic properties depends upon the braid angle. Second, it calculates the nonlinear pre-damage extensional, flexural, and (simple) shear response of a family of geometrically similar triaxial braided composites and compares the calculated macro stress-strain responses with experimental data for a subset of loadings and materials. The differences between the simulated and experimental responses are used to infer the mechanisms responsible for the observed nonlinear macro behavior.

DISCUSSION OF REPRESENTATIVE VOLUME ELEMENT

The RVE is shown schematically in Figure 1 and is similar to those used in [4-6]. The RVE contains two flat 0^o axial tows, two pairs of piecewise linear undulating braider tows oriented in the $+\theta$ and the $-\theta$ directions, and several resin pockets. The tows are braided in a 2 X 2 pattern and have rectangular cross sections to preserve their expansive characteristics. The $\pm\theta$ braider cross over junction is offset from the braider-axial tow cross over junction. The RVE geometry is defined by w, the spacing between axial tows, θ, the braider angle, and $t\,(=t_a + t_b)$, the lamina

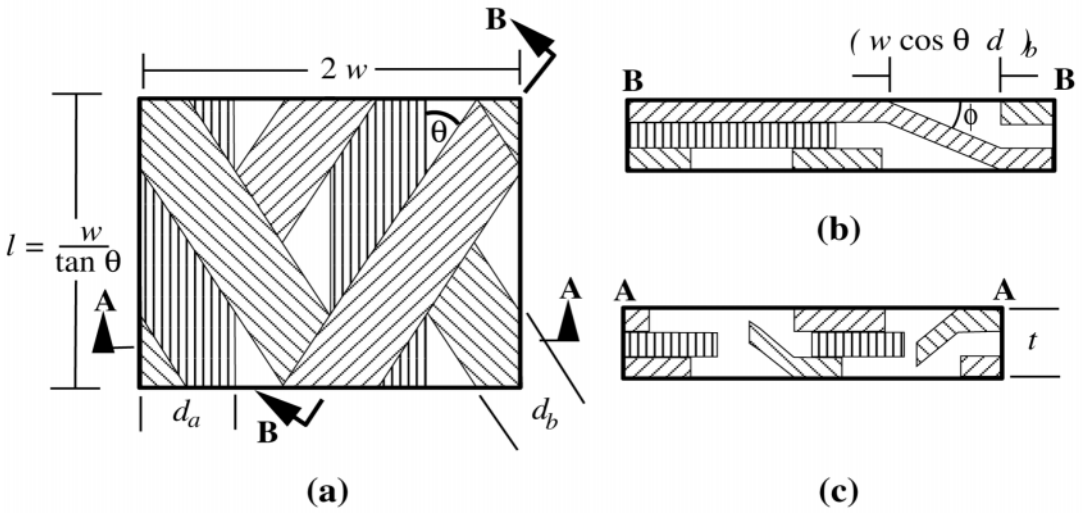

Figure 1. The unit cell: (a) planar view, (b) cross section perpendicular to +θ braider, and (c) cross section perpendicular to axial tow

thickness. Here t_a and t_b are the tow thicknesses, and the subscripts a and b denote axial and braider tow quantities, respectively. The individual tow packing density (fiber volume fraction), p, is determined from the tow width, d, the number of filaments per tow, m_f, and the filament diameter, d_f, as

$$d = \frac{m_f \, d_f^{\,2} \pi / 4}{p \, t}. \tag{2}$$

The crimp angle ϕ depends strongly on the braider width and tow thicknesses, and is given by

$$\phi = \tan^{-1} \frac{\left(t_a + t_b\right) \cos\left(\pi/2 - 2\theta\right)}{w \cos\theta - d_b} \tag{3}$$

The RVE idealization requires that $d_a \le w/2$ and $d_b \le w\cos\theta$ for the braider tows to undulate.

The RVE simplifies the microstructure in several significant ways. Undulations are absent in the axial tows. The piecewise linear idealization of the braider tows

TABLE I. RVE DIMENSIONS AND CRIMP ANGLE

θ	t (mm)	t_b (mm)	d_b (mm)	l (mm)	ϕ
30°	1.550	0.467	6.647	17.60	23.5°
45°	1.753	0.569	5.462	10.16	34.5°
60°	2.286	0.836	3.721	5.866	42.7°

TABLE II. ELASTIC FIBER AND TOW PROPERTIES

	E_l (GPa)	E_t (GPa)	G_{lt} (GPa)	ν_{lt}	ν_{tt}
Fiber	234.3	34.5	24.1	0.300	0.400
Tow	176.5	10.8	5.01	0.315	0.520

yields an overly large crimp angle (for higher fiber volume fractions), a discontinuous fiber direction, and appreciable resin regions surrounding the undulations. Consequently, neither tow representation depicts the true meandering geometry of the fibers. The tows and resin boundaries appear pronounced and rather abrupt compared to the dense melded appearance actually observed in micrographs. Furthermore, only resin exists above and below the braider undulations.

Three similar tri-axially braided carbon fiber polymeric matrix composites are considered. In each, the axial and braider tows contain 80,000 filaments (m_f) with an average fiber diameter of d_f= 6.2 μm. The overall RVE fiber volume fraction is approximately 50%, while the packing fraction in each tow is 75%. The axial fiber spacing (w) is 10.16 mm which yields an RVE width ($2w$) of 20.32 mm. To minimize the crimp angle, d_a is set at 5.08 mm ($w/2$), and thus from (2), t_a is found to be 0.613 mm. Table 1 summarizes the other pertinent RVE dimensions for each composite examined.

The resin material is modeled as an elastic-plastic solid with J-2 power law hardening. It has a Young's modulus of 4.35 GPa, a Poisson's ratio of 0.36, and a flow stress, σ_f, given by σ_f=117.1($\bar{\varepsilon}^p$ + 5X10^{-4})$^{0.04}$ MPa, where $\bar{\varepsilon}^p$ is the equivalent plastic strain. Table 2 lists the transversely isotropic Young's moduli (E_l and E_t), shear modulus (G), and Poisson's ratios (ν) of the fiber, obtained from product literature and data for similar carbon fibers, and of the tow. (The subscripts l and t denote the longitudinal and transverse directions, respectively.) The elastic-plastic tow response is constructed from the resin and fiber behavior and packing fraction using a simple micromechanical model that employs an iso-strain assumption in the fiber direction and a modified iso-stress assumption in the other directions [7].

Three-dimensional FE simulations are performed with NIKE3D, a nonlinear implicit FE code. In each case the RVE is discretized with 8992 8-node selectively reduced, incompatible mode, hexahedral elements such that tow boundaries coincide with element faces. While the meshes do not contain any irregular shaped

TABLE III. EFFECTIVE RVE EXTENSIONAL AND FLEXURAL ELASTIC COEFFICIENTS

	Extensional				Flexural		
θ	E_l (GPa)	E_t (GPa)	ν_{lt}	G_{lt} (GPa)	E_l (GPa)	E_t (GPa)	ν_{lt}
30^o	59.8	8.83	1.07	11.0	32.5	8.37	0.947
45^o	40.0	14.8	0.686	11.5	15.1	12.5	0.631
60^o	29.8	25.9	0.301	8.48	9.01	23.5	0.283

elements in the plane, wedge elements are used in the resin above and below the braider undulations, and slide surfaces are used to constrain the undulation sides to the adjacent mesh. Using the constraints and procedure described in [3], pseudo-periodic displacement boundary conditions are imposed to determine the in-plane elastic extensional, shear, and flexural coefficients. The corresponding nonlinear "uniaxial" responses are obtained by modifying the linear boundary conditions imposed on the adjacent rigid shells.

ELASTIC CHARACTERIZATION

Table 3 summaries the RVE in-plane elastic extensional and flexural properties. In all cases, the coupling matrix and the extension-shear coefficients are four or more orders of magnitude smaller than the other terms. Thus, these quantities are presumed to be zero due to the symmetry of the non-undulating portion of the braider tows. As expected, tow orientation strongly influences the directional extensional and flexural moduli, i.e., as θ increases, E_t increases and E_l decreases. Also, the flexural coefficients are always smaller than their extensional counterparts. The ratio of flexural to extensional Young's modulus is between 0.30 and 0.52 in the longitudinal direction, but only between 0.90 and 0.95 in the transverse direction. Clearly, the distance from the braider to the mid-surface has a significant impact on this result.

Experimental Measurements of Elastic Properties

A series of extensional and flexural tests were performed to experimentally measure the longitudinal properties of the $0/\pm 30^{o}$ composite. As described in [3], five rectangular specimens 38.1 mm by 250.4 mm were machined from a 3.10 mm thick 2-ply composite plate. Strain gauge rosettes, 6.35 mm by 25.4 mm, were applied on the front and back specimen surfaces at the same location. The specimens were first loaded in uni-axial tension to 0.5% strain. The stress strain curve remained linear after the initial seat-in period. Next, the samples were tested in flexure with a 4-point bend fixture. The minor and major spans measured 63.5 mm and 190.5 mm, respectively. Each specimen was tested, unloaded, flipped over, and re-tested to generate a consistent set of load-deflection traces.

Due to large-scale tow movement during molding, the number of axial tows per

TABLE IV. MEASURED AND FE-BASED YOUNG'S MODULI AND POISSON'S RATIOS FOR A $0^{o}/\pm 30^{o}$ BRAIDED COMPOSITE

	Experimental						FE
Specimen	1	2	3	4	5	Average	
E_l (GPa)	55.7	51.5	38.8	64.6	57.7	53.7	59.81
ν_{lt}	1.06	1.21	1.11	1.17	1.31	1.17	1.07
E_{lam}/E_l	0.728	0.808	0.804	0.671	0.898	0.782	0.849

unit length, q, varied significantly between specimens. A full width slice of each specimen was removed immediately below the strain gauges, measured, and subjected to a 4 hour 400° C burn-out procedure. (A section of the raw fiber was subjected to the same procedure to determine the fiber mass lost.) The 0° fibers were then collected and weighed. After adjusting for mass loss, q for each specimen was determined.

Table 4 contains the measured values of the extensional E_l and ν_{lt}, and the ratio of E_{lam}, the effective longitudinal direction flexural Young's modulus of the laminate, to E_l for each specimen. Since E_l depends strongly upon q, the quantity E_l/qw is presented in an attempt to normalize the data for variations in q. (The term qw represents the ratio of the theoretical value of q, $(1/w)$, to the measured value of q.) For comparison purposes, the FE based values are also listed as well as an estimate of E_{lam}/E_l obtained from (1) using the FE results.

NONLINEAR MACRO RESPONSE

The extensional, bending, and simple shear responses were simulated. Uniaxial stress was imposed in the longitudinal and transverse directions for each braider angle. A nondimensional stress was defined as the macro stress divided by the macro elastic stress Σ_e, calculated as $\Sigma_e = E\varepsilon$, where E is the corresponding RVE extensional Young's moduli and ε is the imposed macro strain. Figures 2 and 3 show the Σ_e versus strain curve in the longitudinal and transverse directions, respectively. The figures include two experimental curves for a $0^o/\pm 30^o$ braided composite similarly normalized. (Normalization with Σ_e renders the onset of nonlinear behavior obvious.) The shear response, obtained under "simple shear" conditions (no macro longitudinal strain), is plotted in Figure 4. Uniaxial bending, without anticlastic curvature suppression, was examined about the two primary

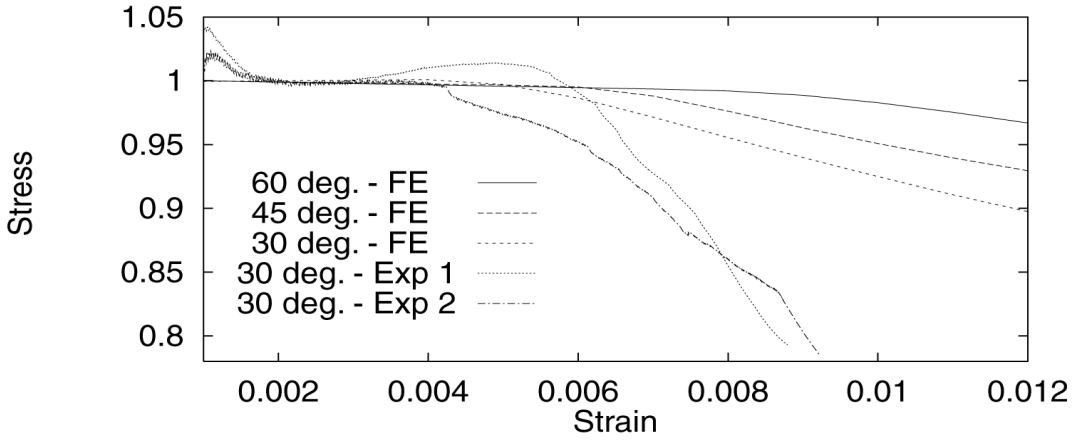

Figure 2. Normalized longitudinal stress-strain curves from tests on a $0^o/\pm 30^o$ braided composite and various FE simulations

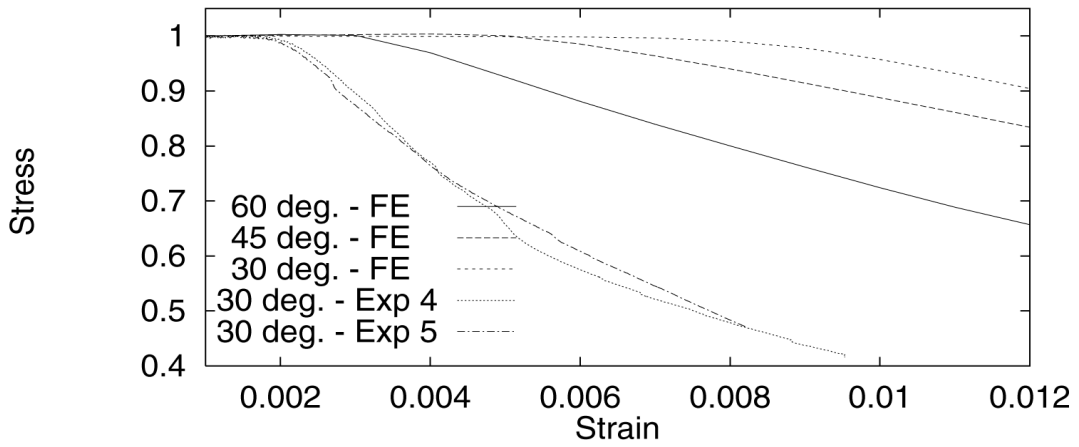

Figure 3. Normalized transverse stress-strain curves from tests on a $0^o/\pm 30^o$ braided composite and various FE simulations

axes. Figure 5 shows the normalized bending moment, defined as the macro moment divided by the macro elastic moment M_e, versus the upper surface macro strain for rotations imposed about the longitudinal (Long.) and transverse (Tran.) axes. (M_e is given by $M_e = 2EI\varepsilon/t$, where E and I are the corresponding flexural Young's modulus and moment of inertia, respectively.) While regions of modest plasticity develop in the RVE for all loadings, this is not always apparent from the macro stress-strain or moment-strain curves.

For the $0^o/\pm 30^o$ braid, the predicted onset of macro yield in uniaxial extension coincides with the experimental values in the longitudinal direction, while it is nearly twice the experimental values in the transverse direction. This suggests that softening arises in the longitudinal direction, at least initially, from plastic deformation rather than damage where as the opposite appears true in the transverse direction. In simple shear, diffuse matrix plasticity around the undulations accommodates the braider rotations and out-of-plane displacement of the middle

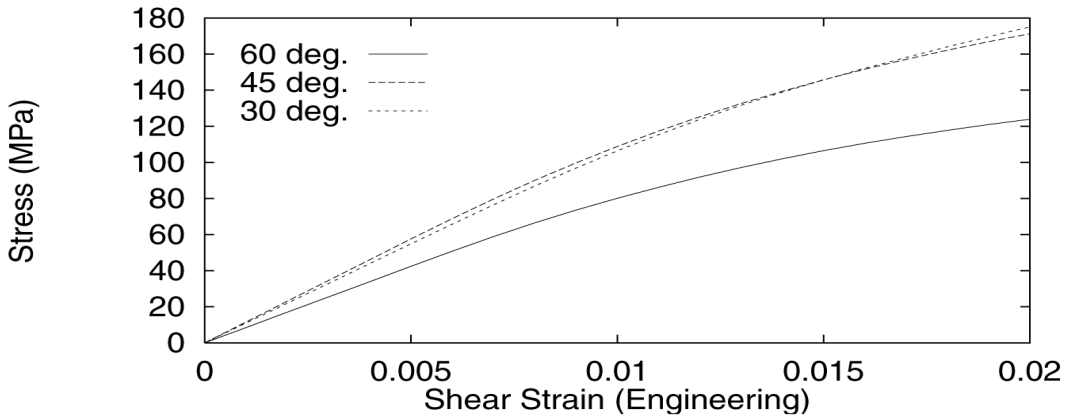

Figure 4. Shear stress versus shear strain (engineering) curves

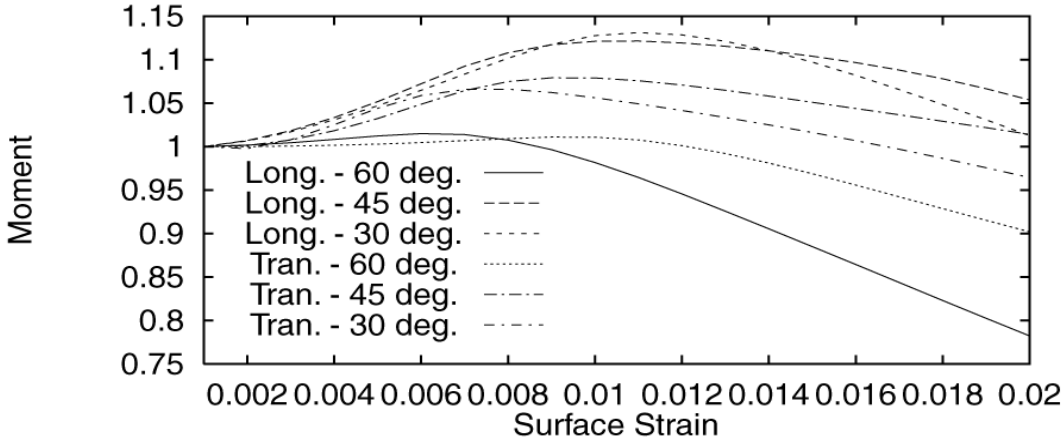

Figure 5. Normalized bending moment versus macro upper surface strain

RVE half (relative to the outer edges) after macro yield. Under uniaxial flexure, moderate stiffening occurs prior to strain softening in both the principal directions. Clearly, the behaviors observed require additional investigation to fully understand their consequences.

ACKNOWLEDGMENTS

This work was performed under the auspices of the U.S. D.O.E. by Lawrence Livermore National Laboratory under contract W-7405-Eng-48 and was supported by the U.S. D.O.E., Office of Transportation Technologies, Lightweight Material Program under Dr. J. Carpenter and Mr. D. Warren. The authors appreciate the material and interactions provided by the Automotive Composite Consortium.

REFERENCES

1. Marrey, R. V. and B. V. Sankar. 1997. “A Micromechanical Model for Textile Composite Plates,” *J. Comp. Matls*., 31(12):1187-1213.
2. Whitcomb, J. D., C. D. Chapman, and K. Srirengan. 1998. “Analysis of Plain Weave Composites Subjected to Flexure,” *Mech. Comp. Matls. Struct*., 5(1):41-53.
3. Zywicz, E. and T. Nguyen. 1999. “On the Flexural and Extensional Behavior of a Large-Tow Triaxial Braided Composite,” to appear in *Comp. Sci. Tech.*
4. Dadkhah, M. S., J. G. Flintoff, T. Kniveton, and B. N. Cox. 1995. “Simple Models for Triaxially Braided Composites,” *Composites*, 26(8):561-577.
5. Carrier, C. R., and R. C. Averill, 2000. “A Simple Discrete-Tow Model for Analysis of Textile Composites,” to appear in *Comp. Tech. Res.,* 22(4*).*
6. Naik, R. A. 1995. “Failure Analysis of Woven and Braided Fabric Reinforced Composites.” *J. Comp. Matls*., 29(17):2334-2363.
7. Nukala P. K., J. Y. Shu, and E. Zywicz. 1999. “A Three-Dimensional Finite Deformation Couple Stress Model for Fiber-Reinforced Composites,” LLNL Report UCRL-JC-134374, University of California, Livermore.